Journal of Physics:
Conference Series

PAPER • **OPEN ACCESS**

Exploring the Kipenhahn-Schlüter model

To cite this article: Carlos D. Vigh *et al* 2018 *J. Phys.: Conf. Ser.* **1031** 012012

IOP Conf. Series: Journal of Physics: Conf. Series **1031** (2018) 012012 doi:10.1088/1742-6596/1031/1/012012

Exploring the Kipenhahn-Schlüter model

Carlos D. Vigh,[123] Rafael Gonzalez,[4] and Diego Rial[5]

[1]Instituto de Ciencias, Universidad Nacional de General Sarmiento, Los Polvorines, Buenos Aires, Argentina;
[2]Universidad de Buenos Aires. Facultad de Ciencias Exactas y Naturales. Departamento de Física. Buenos Aires, Argentina;
[3]CONICET-Universidad de Buenos Aires. Instituto de Física del Plasma (INFIP). Buenos Aires, Argentina;
[4]Instituto de Desarrollo Humano, Universidad Nacional de General Sarmiento, Los Polvorines, Buenos Aires, Argentina;
[5]Universidad de Buenos Aires. Facultad de Ciencias Exactas y Naturales. Departamento de Matemática. Buenos Aires, Argentina;

E-mail: cvigh@ungs.edu.ar

Abstract. We explored the generalised Kippenhan-Schlüter model non-isothermal stationary states for solar prominences where we made some improvements. The most important is to use recent observed values of radiative losses to build the piecewise heat balance equation. We explicity found several stationary states without and with magnetic shear solutions for the system of equations in the beta plasma range between 0 and 1,6. Finally, we computed magnetic streamlines field for the different shears. Joining all these elements we obtained a catalogue to study the stability of the prominence candidates.

1. Introduction

Quiescent solar prominences are structures extended into the solar corona, are denser and colder than coronal neighborhood. They have a small width compared to their length and height. Also, they have lifetimes from minutes to months and present relative small velocity flows. Therefore it implies that structures must be close to energy balance equilibrium [1]. The magnetic field is one of the agents of thermal isolation respect its environment [2]. Costa et al. [3] made an stability analysis using thermodynamic irreversible energy principles for different solar ambients (For examples, see [4] and [5]). The goal in that work was extend and generalize the MHD energy principle of Bernstein [6] using a general procedure considering irreversible thermodynamics processes where Bernstein's principle is a particular case. This method includes dissipation and it shows explicitly the contributions of radiation, heat mechanisms and magnetic energy (see equations 36 and 37 in [3]). Applied this method to solar prominences shows an alternative point of view to understand which mechanisms participates into its developing and stability structure. Recently, several works used the isothermal Kippenhan-Schlüter (KS) model [7] to study the prominence dynamics where were performed numerical simulations and compared with observations. (To see some examples [8], [9], [10], [11] and [12]) In particular, Costa et al [3] used this general energy principle onto the isothermal KS model to study oscillation wave modes. In this way is possible to identify which is the relative importance between different sources like radiation and thermal heating and also is possible to compare with observational

data periods corresponding to typical oscillation of the cromosphere and photosphere which can be explained as internal prominence modes. A natural extension of that work is to examine the non-isothermal case, *i.e.* the Generalized Kippenhan-Schlüter model (KS-G). The KS-G model has the advantage to bring solutions into a wide range of β plasma. This variation of β allows to determine the relevance of the different contributions to the prominence stability and its internal wave modes *i.e. magnetic energy, thermal heating and radiative losses*, comparing for example, with force-free models (low β range) where is most difficult to identify it. To do this, it is necessary to recompute previous results of this simple model upgrading and revalidating the dynamical solutions of KS-G model for quiescent prominences. In that way, in a next work, will be possible to study stability and modal structure corresponding to perturbations from the equilibria using the appointed sources before. According the beta plasma definition, Milne et al. [13], [14] found that in the range 0 and 1.6 exists stationary solutions for different heating functions models. For a better description we took sixteen regions cooling of radiative values from recent works [15] and recompute profiles of temperature, density, pressure and magnetic fields. We extend the analysis to the whole range $-1 \leq x \leq 1$ checking the symmetry of the solutions. Finally, we computed the magnetic field streamlines. This is a working progress where the next stage of our project will be recompute the variational principle using the collection of solutions obtained here to generalize the aforementioned study.

1.1. Kippenhahn-Schlüter Model

Following Milne et al. [13] we worked onto the extension of Kippenhahn-Schlüter model taking into account thermal effects. For convenience we used the set of equations in adimensional form. Firstly, the equations that describes balance between hydrostatic, gas and magnetic pressure in a stationary regime are

$$\beta \frac{dp}{dx} = -2B_z \frac{dB_z}{dx} \tag{1}$$

$$\frac{dB_z}{dx} = \frac{1}{2}\beta\rho \tag{2}$$

where $\beta = 2\mu p_1/B_0^2$ is the "beta" plasma, being the characteristical pressure is $p_1 = 1.67 \times 10^{-13}\mathrm{Kg/m^3}$. μ is the magnetic permeability. B_0 is the characteristical magnetic field in the x coordinate, p is the gas pressure and B_z the magnetic field in the z direction as shown in Figure 1. Pressure p and temperature T are related by the state equation of an ideal gas

$$p = \rho T \tag{3}$$

The heat balance between mechanical heating, radiation losses and thermal conductivity is

$$\frac{d}{dx}\left(\frac{T^{5/2}}{B^2}\frac{dT}{dx}\right) = C\rho^2 T^{\alpha} - C_1(T)\rho \tag{4}$$

Finally, the magnetic field is:

$$B^2 = 1 + B_y^2 + B_z^2 \tag{5}$$

where B is the magnetic field in cartesian coordinates, using as normalization $B_x = B_0$. By other way x is the normalized position, being $x = 0$ at the prominence center and $x = 1$ its external boundary in the solar corona. ρ, is the gas density and T the temperature.
The constant C is defined like:

$$C = \frac{\chi\ p_1^2\ T_1^{\alpha-3.5}}{g^2\ \kappa} \tag{6}$$

Table 1. Values of radiative losses from CHIANTI using sixteen cooling regions [15]

Temperature (K)	χ	α
$T < 1.26 \times 10^4$	2.02×10^{-15}	8.06
$1.26 \times 10^4 \leq T < 1.58 \times 10^4$	5.60×10^{-2}	4.78
$1.58 \times 10^4 \leq T < 2.51 \times 10^4$	1.36×10^{24}	-1.26
$2.51 \times 10^4 \leq T < 3.16 \times 10^4$	1.46×10^{17}	0.32
$3.16 \times 10^4 \leq T < 7.9 \times 10^4$	3.11×10^{11}	1.58
$7.9 \times 10^4 \leq T < 1.0 \times 10^5$	4.44×10^{16}	0.53
$1.0 \times 10^5 \leq T < 1.25 \times 10^5$	2.31×10^{20}	-0.22
$1.25 \times 10^5 \leq T < 2.0 \times 10^5$	1.44×10^{17}	0.41
$2.0 \times 10^5 \leq T < 2.51 \times 10^5$	1.20×10^{19}	0.05
$2.51 \times 10^5 \leq T < 3.98 \times 10^5$	2.02×10^{27}	-1.47
$3.98 \times 10^5 \leq T < 7.94 \times 10^5$	6.38×10^{17}	0.22
$7.94 \times 10^5 \leq T < 1.0 \times 10^6$	1.40×10^{19}	0.0
$1.0 \times 10^6 \leq T < 2.0 \times 10^6$	1.26×10^{24}	-0.82
$2.0 \times 10^6 \leq T < 3.98 \times 10^6$	4.14×10^{28}	-1.54
$3.98 \times 10^6 \leq T < 1.0 \times 10^7$	7.74×10^{16}	0.23
$1.0 \times 10^7 \leq T < 3.16 \times 10^7$	2.06×10^{25}	-0.98
$T < 3.16 \times 10^7$	3.20×10^{16}	0.20

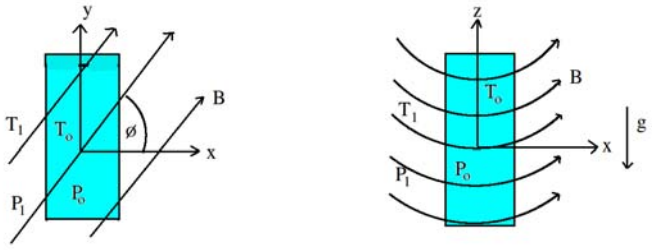

Figure 1. Schematic representation of a prominence. The x-axis is normal to prominence sheet, while the y-axis runs along the length of the prominence. The quantity ϕ is the shear angle between the prominence normal and the horizontal magnetic field. Values at the center are denoted by the subscript 0, while in the external corona are denoted by the subscript 1, see [13].

where T_1 is the characteristical temperature $T_1 = 2 \times 10^6$K, the gravity $g = 274$m/s^2 and the thermal conductivity $\kappa = 3 \times 10^{-11}$. C is a temperature piecewise function and C_1 is:

$$C_1(T) = \begin{cases} 0 & \text{si } T < 0.1; \\ C(T = p = x = 1) & \text{si } T \geq 0.1. \end{cases}$$

We defined a zero heat region near $x \sim 0$, the center prominence and in $x = 1$ we assured no-heat exchange with the external environment. The values of χ and α will be different in each region as shown in the Table 1. This is the most relevant improvement respect the work of Milne et al [13], where they used the Hildner's six regions cooling [16].

1.2. Boundary conditions
To solve the system is necesary to specify β and B_z and also four boundary conditions, the first two are according to maintain the symmetry as shown in Figure 1:

$$B_z = 0 \qquad at\ x = 0 \tag{7}$$

$$\frac{dT}{dx} = 0 \qquad at\ x = 0 \tag{8}$$

The next two conditions are stablished to assure the continuity with the coronal values

$$\rho = 1 \qquad at\ x = 1 \tag{9}$$

$$T = 1 \qquad at\ x = 1 \tag{10}$$

In this way, the shear angle is directly:

$$\Phi = arctg(B_y) \tag{11}$$

2. Semi-analytical solutions

The system equations 1 to 4 constitutes a two-point boundary-value problem, and it has not got analytical solution. Then, it is necessary to solve it numerically. Also, the character of piecewise functions $C_1(T)$ and $\alpha(T)$ inserts into equation 4 strong gradients between cooling regions being a source of numerical errors. Another source of troubles is that the model we are using is not valid beyond $x = 1$ where vertical variations become important [13]. This system could be solved via Runge-Kutta method building an elementary code or using numerical solvers tools for ODE equations [17]. The boundary conditions are fullfiled by shooting, it means, fixing ρ_0 and T_0 at $x = 0$ and varying β and B_y until satisfy the boundary conditions at $x = 1$. This strategy is easy and fast to obtain the collection of solutions that we are searching for a theoretical comprehension explained in the Introduction. Increase a 3D model requires a more sofisticated tool. In this way it is possible to obtain *temperature, magnetic field, pressure and density.* Also, compare and check it with semi-analytical expressions it is important (see equations 11 and 12 in [13]). Therefore, we took the temperature profile from the numerical solution and we use it as input for the following analytical expressions.

$$\frac{dB_z}{dx} - \frac{1}{2}\frac{\beta p}{T} = 0 \tag{12}$$

$$\frac{d}{dx}\left(T\frac{dB_z}{dx}\right) + \frac{d}{dx}\left(\frac{1}{2}B_z^2\right) = 0 \tag{13}$$

Then, the solutions are:

$$B_z(x) = \sqrt{\beta p_0}\ tanh\left[\frac{1}{2}\ell(x)\sqrt{\beta p_0}\right] \tag{14}$$

$$p(x) = p_0\ sech^2\left[\frac{1}{2}\ell(x)\sqrt{\beta p_0}\right] \tag{15}$$

where

$$\ell(x) = \int_0^x \frac{dy}{T(y)} \tag{16}$$

If $T = 1$ we recover the Kipenhahn-Schlüter model (1957).

Left: Numerical pressure profiles. **Right:** semi-analytical pressure profiles.

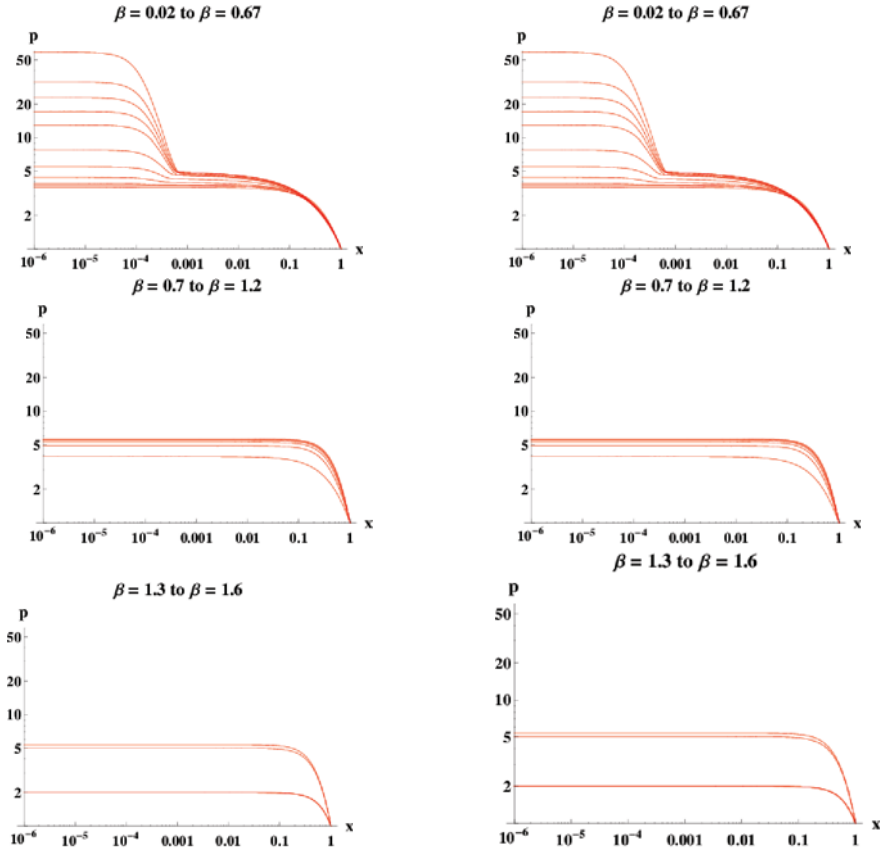

Figure 2. Top: β is in the range $[0.02-0.67]$, inferior curves, lower β, upper curves, higher values. Experiments are setted as β= 0.02; 0.04; 0.06; 0.08; 0.1; 0.2; 0.3; 0.4; 0.5; 0.6 y 0.67 from bottom to top curves. **Medium:** β= 0.7; 0.8; 0.9; 1.0; 1.1 y 1.2. The qualitative change is for $\beta = 0.7$, values greater that 0.8, tends to isothermic behaviour. **Bottom:** β: 1.3; 1.4; 1.5 and 1.6.

3. Checking consistency

We checked numerical and semi-analytical solutions comparing between different β, here we present the pressure evolution. Also for convenience, the profiles are in the range $0 \leq x \leq 1$, but the solutions are completely symmetric in the range $-1 \leq x \leq 0$.

3.1. Numerical setting

In Table 2 we showed the input values to set the experiments and the outputs in the boundaries. If we divided the values of T_0 in cold ($T \leq 0.1$) and hot solutions ($T \geq 0.1$), we noted that for higher shears the stationary states corresponds to hot solutions.

3.2. Pressure Evolution

We divided the solutions in three ranges, at the top of Figure 2 solutions for $0.02 < \beta < 0.67$, at medium of Figure 2 for $0.7 < \beta < 1.2$, and at the bottom for $1.3 < \beta < 1.6$. We noted a qualitative change of behaviour around $\beta = 0.67$ for higher values the profiles tends to isothermal solutions.

Table 2. Input and outputs values of the numerical experiments.

By	β	T_0	p_0	$p(1)$	$T(1)$	$Bz(1)$
0	0.02	0.000081	58.4	1.00684	1.00611	1.07138
0	0.6	0.00136	3.595	1.00125	1.00195	1.2475
0	1.6	0.999999	2.000	0.98292	1.00326	1.27567
0.5	0.025	0.000089	42.12	1.00784	0.99481	1.01387
0.5	0.6	0.001045	3.593	1.00093	1.00997	1.24709
0.5	1.6	0.999	2.12	1.00245	1.00394	1.33719
5.8	0.025	0.000175	1.2	1.00555	1.02614	0.0697222
5.8	0.6	0.47	1.51	1.00443	1.00085	0.550763
5.8	1.6	0.935	2.3	1.00233	1.05758	1.44093
10	0.025	0.54	1.03	1.018	1.005	0.017
10	0.6	0.73	1.31	1.007	1.011	0.426
10	1.6	0.95	1.9	0.985	1.118	1.21

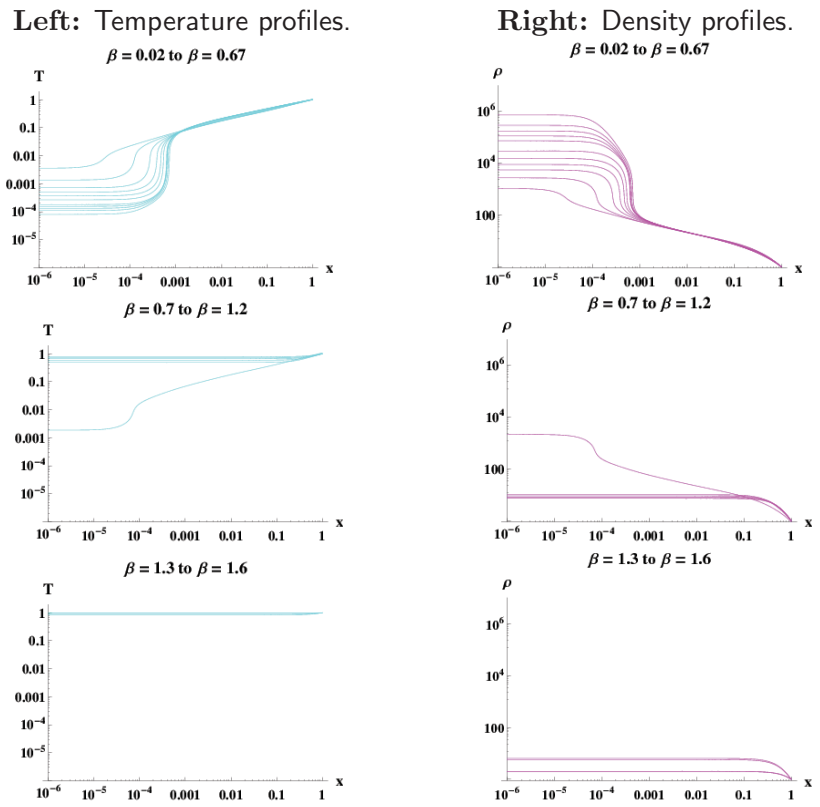

Figure 3. Top: left, temperature and right, density. β is in the range $[0.02-0.67]$, inferior curves, lower β, upper curves, higher values. Experiments are setted as β= 0.02; 0.04; 0.06; 0.08; 0.1; 0.2; 0.3; 0.4; 0.5; 0.6 y 0.67 from bottom to top curves. **Medium:** β= 0.7; 0.8; 0.9; 1.0; 1.1 y 1.2. The qualitative change is for $\beta = 0.7$, values greater that 0.8, tends to isothermic behaviour. **Bottom:** β: 1.3; 1.4; 1.5 and 1.6.

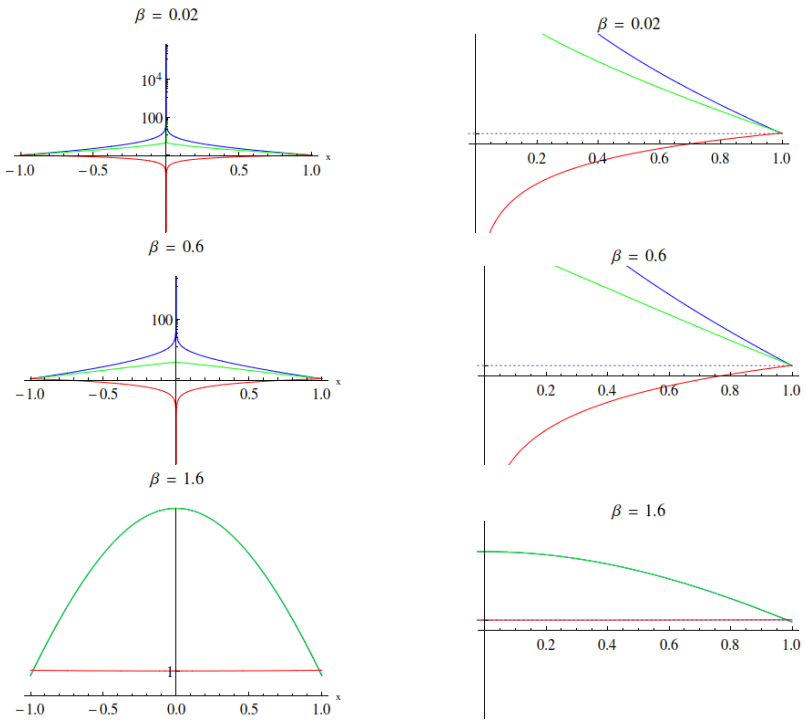

Figure 4. Left: Density (blue), pressure (green) and temperature (red) profiles.**Right:** Same magnitudes near $x = 1$.

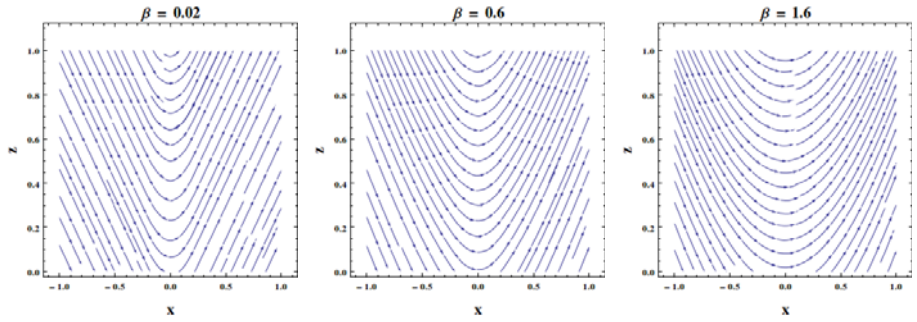

Figure 5. Magnetic field streamlines with $B_y = 0, \Phi = 0$

3.3. Profiles of Temperature and Density

In Figure 2 we checked that the semi-analytical and numerical solutions have a good degree of coincidence. In the Figure 3 we showed the corresponding profiles of temperature and density for different values of β. Here is possible to see explicitly that the solutions are consistent with the fact that prominences are denser and closer in its interior.

3.4. Checking the state equation of an ideal gas

Last quality test is to check boundary conditions and the state equation for an ideal gas. Here we selected for $\beta = 0.02, 0.6$ and 1.6; we showed for the whole range for values of x in the Figure 4 (left) and near the boundaries (right) where the boundary conditions are fulfilled numerically.

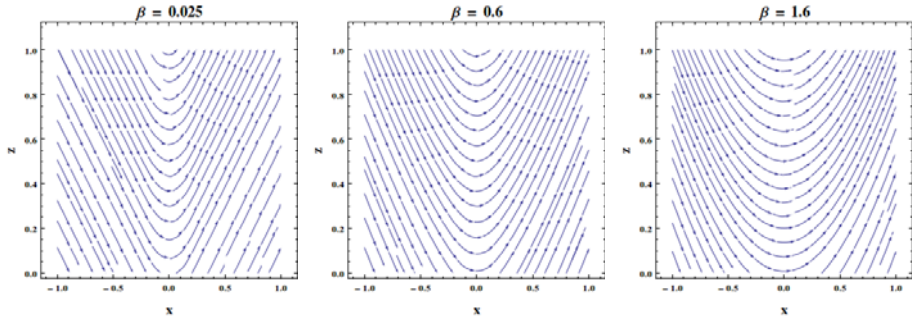

Figure 6. Magnetic field streamlines with $B_y = 0.5, \Phi = 28^o$

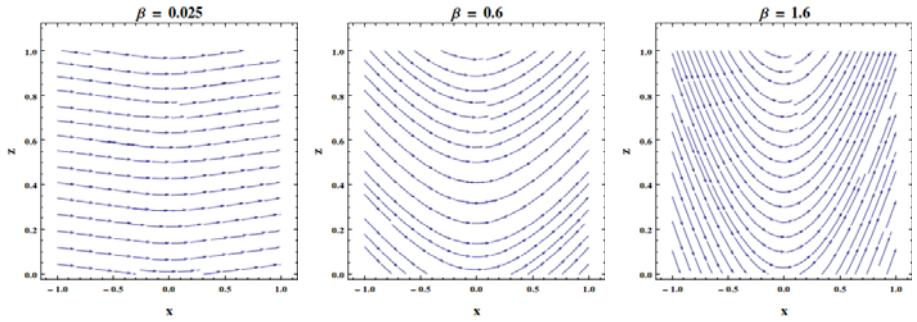

Figure 7. Magnetic field streamlines with $B_y = 5.8, \Phi = 80^o$

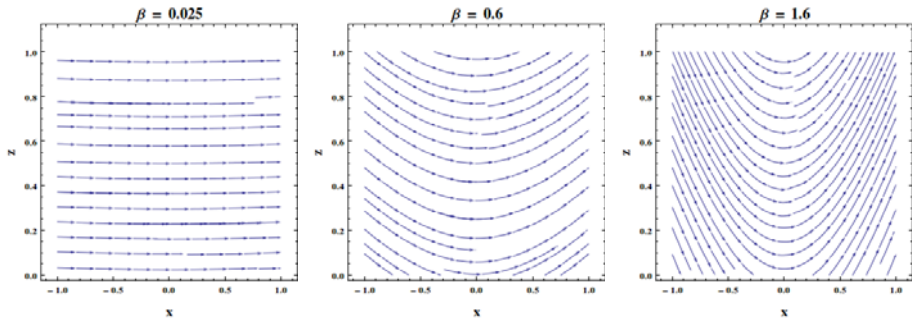

Figure 8. Magnetic field streamlines with $B_y = 10, \Phi = 84^o$

4. Magnetic field streamlines for non-isothermal cases

We selected for three values of β different magnetic shears to see how to affect the magnetic field streamlines. $\Phi = \{0^o, 28^o, 80^o, 84^o\}$ which corresponds respectively to $B_y = \{0, 0.5, 5.8, 10\}$ The Figure 5 is the reference case without shear, the behaviour of streamlines increasing β is qualitative similar. However, in the Figures 6, 7 and 8, we can see when the shears increase, the streamlines tends to alligned into direction $\hat{y}$. The case $\beta = 0.025$ is the most sensitive to change with shear. For $\beta = 0.6$, we have change with shear too, but is lower respect to $\beta = 0.025$. Finally, for $\beta = 1.6$ the effect is weak comparing the another two cases.

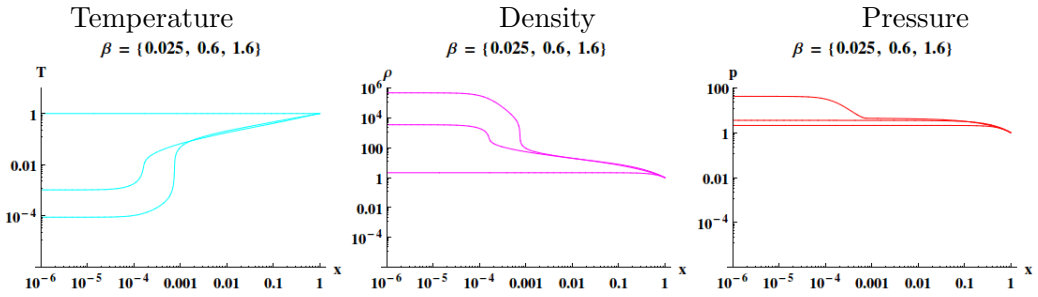

Figure 9. Case $B_y = 0.5, \Phi = 28^o$. For the temperature lower curve is for $\beta = 0.025$, intermediate curve for $\beta = 0.6$ and upper one for $\beta = 1.6$. For density and pressure the curves are upper $\beta = 0.025$, intermediate $\beta = 0.6$ and lower $\beta = 1.6$.

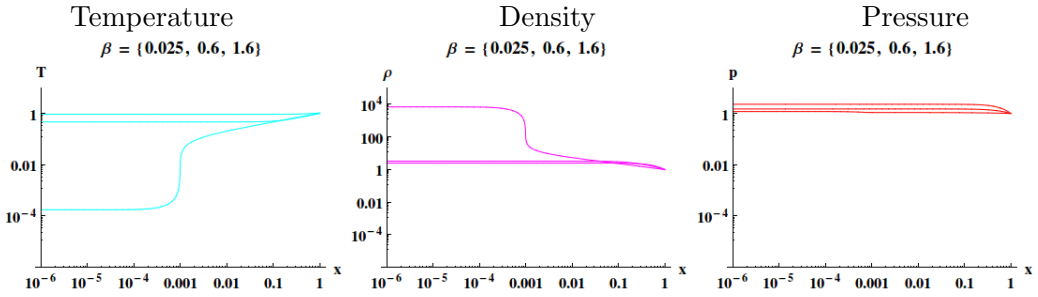

Figure 10. Case $B_y = 5.8, \Phi = 80^o$. For the temperature lower curve is for $\beta = 0.025$, intermediate curve for $\beta = 0.6$ and upper one for $\beta = 1.6$. For density and pressure the curves are upper $\beta = 0.025$, intermediate $\beta = 0.6$ and lower $\beta = 1.6$.

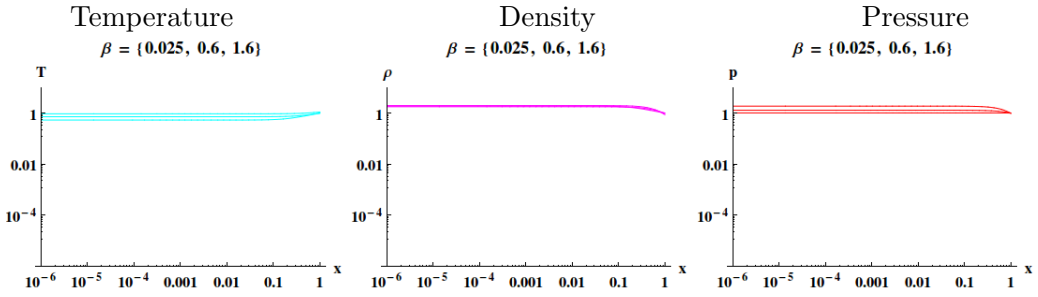

Figure 11. Case $B_y = 10, \Phi = 84^o$. For the temperature lower curve is for $\beta = 0.025$, intermediate curve for $\beta = 0.6$ and upper one for $\beta = 1.6$. For density and pressure the curves are upper $\beta = 0.025$, intermediate $\beta = 0.6$ and lower $\beta = 1.6$.

4.1. Temperature, density and pressure profiles for different shears

In this paragraph we saw how the shear affects temperature, density and pressure profiles for the same values of β. The case $B_y = 0$ is shown in subsection 3.4. From Figures 9, 10 and 11 is clear that for $\beta = 0.025$ is the most sensitive for the change of shear. More specifically when increase the shear the system has a tendency to be isothermic.

5. Conclusions and next steps

In this work we explored for Kippenhan-Schlüter model extended to non-isothermal stationary states. We upgraded the piecewise heat equation according the values of Table 1. For these reason we used recent observed values to improve the heat equation subdividing in sixteen cooling regions in place to six cooling regions due to Hildner's values. Before to make the numerical experiments for several cases we checked consistency between analytical and semi-analytical solutions. After that, we began to analyse the behaviour of different profiles for several values of β, in this way we explicitly showed temperature, density and pressure profiles. We found several stationary states without and with magnetic shear solutions for the system of equations in the β range between 0 and 1.6 which corresponds to solar prominences. Beyond this value of β we can not find stationary solutions which satisfies boundary conditions in the solar corona.

After that, we selected for $\beta = 0.025, 0.6$ and 1.6 cases to study the behaviour of magnetic field streamlines for different magnetic shears. In all cases the increasing of shear modifies the streamlines tends to allign in the y direction. The case $\beta = 0.025$ is the most sensitive with the change of shear.We obtain non-isothermal solutions for values of β lower than 0.7, meanwhile for higher values ($\beta > 0.7$) solutions corresponds to Kippenhan-Schlüter isothermic model and it is independent of the shear.

By another way, if B_y component of magnetic field is higher than B_x the system will have a tendency to be isothermic, independently of the values of β.

This work is a first step to perform a catalogue to analyse the stability of this kind of structures using variational principles. Joining all these elements we have a catalogue to study in a next stage of our project the stability of the prominence candidates in this minimalistic unidimensional context.

Acknowledgments

CV is grateful for partial financial support of Instituto de Ciencias, UNGS, Los Polvorines.

References

[1] Anzer U and Heinzel P 1999 *Astron.Astrophys.* **349** 974–984
[2] Galindo-Trejo J 2006 *RMxAA* **42** 89–98
[3] Costa A, González R and Sicardi-Scifino A 2004 *Astron.Astrophys.* **427** 353–361
[4] Costa A and González R 2006 *Astron.Astrophys.* **458** 953–963
[5] Costa A and González R 2008 *Astron.Astrophys.* **489** 755–762
[6] Bernstein I, Frieman E, Kruskal M and Kulsrud R 1958 *Proc.Roy.Soc A* **244** 17
[7] Kippenhahn R and Schlüter A 1957 *Zs.Ap.* **43** 36
[8] Hillier A, Isobe H, Shibata K and Berger T 2011 MHD simulations of quiescent prominence upflows in the Kippenhahn-Schlüter prominence model *Astronomical Society of India Conference Series* (*Astronomical Society of India Conference Series* vol 2) ed Chouduri A and Banerjee D pp 331–336
[9] Petrie G and Low B The internal structures and dynamics of solar quiescent prominences *Astronomical Society of the Pacific Conference Series* Astronomical Society of the Pacific Conference Series
[10] Low B and Petrie G 2005 *ApJ* **626** 551–562
[11] Hillier A, Shibata K and Isobe H 2010 *Publ.Astron.Soc.Japan* **62** 1231–1237
[12] Hillier A, Isobe H, Berger T and Shibata K 2012 *ApJ* **746** 120
[13] Milne A, Priest E and Roberts B 1979 *ApJ* **232** 304
[14] Priest E 1982 *Solar Magnetohydrodynamics* 4th ed (*Geophysics and Astrophysics Monographs* no 21) (Dordrecht, Holland: Kluwer Academic Publishers)
[15] Soler R, Ballester J and Parenti S 2012 *Astron.Astrophys.* **540** id.A7,6pp.
[16] Hildner E 1974 *Solar Phys.* **35** 123
[17] Wolfram 2014 *Mathematica* version 10.0 ed (Champaign, Illinois: Wolfram Research, Inc)